International Journal of Bridge Engineering (IJBE), Special Issue 2017, pp. 171-189

SEISMIC REPAIR DESIGN OF RC BRIDGE COLUMNS DAMAGED UNDER COMBINED BENDING AND TORSION EFFECTS

Yang Yang[1], Ruili He[2] and Lesley Sneed[3]

[1] University of Hartford, Dept. of Civil, Environmental, and Biomedic Engineering, West Hartford, Connecticut, USA
[2] Garver, LLC, Kansas City, Missouri, USA
[3] Missouri University of Science and Technology, Dept. of Civil, Architechtural, and Environmental Engineering, Rolla, Missouri, USA
e-mail: yyang@hartford.edu, RHe@garverusa.com, sneedlh@mst.edu

ABSTRACT: As a major energy dissipating component, reinforced concrete (RC) bridge columns may experience damage such as concrete cracking, concrete crushing, reinforcing steel yielding, or even reinforcing steel fracture in a severe earthquake. For bridges with irregular configurations (skewed, curved, or having outrigger bent beams), the columns can be subjected to combined bending and torsion effects during earthquakes, and the damage conditions differ from those of columns subjected to bending alone. Rapid repair of these columns in a short timeframe is critical to enable rescue efforts and the quick reopening of the bridge to emergency vehicles after earthquakes; thus, repair design guidelines that can be quickly adopted by engineers are needed for the combined loading conditions, although most researchers have focused on columns under bending effects only. This paper summarizes the current available test data on RC columns damaged under combined bending and torsional loading and develops a unified design procedure for the rapid repair using externally bonded carbon fiber reinforced polymer (CFRP) composite jackets. The design considers the required repair length, the number of layers of the CFRP jacket, and details that are required to effectively transfer loadings between the CFRP and other parts of the columns. Test data from columns before and after repair are compared in terms of strength, stiffness, and ductility and used to validate the design approach and demonstrate its effectiveness for practicing engineers.

KEYWORDS: Bridge columns; earthquakes; carbon fiber reinforced polymer; rapid repair; torsion.

1 INTRODUCTION

During earthquakes, the columns of bridges with irregular configurations may

be subjected to combined axial, flexure, shear, and torsion loadings [1-5]. Although reinforced concrete (RC) bridge columns are not usually designed to resist torsional loading, torsion may occur in skewed bridges, curved bridges, bridges with columns of varied aspect ratios, or bridges with outrigger columns. Torsional loading on RC bridge columns influences the lateral behavior by reducing the lateral strength and deformation capacities, and the torsional strength and deformation capacity also decreases with increasing lateral deformation [6-9]. Thus, the damage conditions of columns subjected to combined loading including torsion differ from those of columns subjected to bending alone.

Damage to bridge structures during an earthquake can have devastating social and economic consequences, particularly for bridges located along key routes that are critical for emergency response and other essential functions. Such bridges are defined as "important" by ATC-18 [10], which stipulates that damage from an earthquake should be repaired within three days. Thus, rapid and efficient repair techniques are required to restore the functionality of the bridge for emergency vehicles to provide timely service and mitigate the impact on the affected community. As such, rapid repair may also be referred as "emergency" repair due to the fact that long term effects are not considered in the repair.

In most repair studies, rapid repair has not been emphasized, and the timely reopening of the structure to traffic has not been a primary consideration. Although various techniques have been shown to be effective in restoring the capacity of damaged RC columns, they generally require considerable time, expert workers, and/or specialized equipment during construction. Therefore, most methods in the literature are difficult to accomplish as part of an emergency rapid repair. Recently, some work has been conducted on rapid repair of RC columns using externally bonded carbon fiber reinforced polymer (CFRP) composites [11-13] and other advanced materials such as shape memory alloys [14-17]. These studies were focused on columns that were damaged under cyclic bending moment and shear, without the inclusion of torsion. Though some studies have focused on torsional strengthening of RC members (e.g., [18-21]), little work [22-26] has been done on rapid repair of RC columns damaged under combined axial, shear, flexural, and torsional loading.

In this paper, RC bridge column repair design is presented in terms of case studies on five columns damaged under combined axial, bending, shear, and torsion effects. The focus of this paper is the repair design methodology, whereas the repair procedure and response of the repaired columns are reported in detail elsewhere [22-24]. The columns were repaired using an externally bonded CFRP composite strengthening system in order to achieve a rapid and effective repair; thus, the design mainly focuses on determining the repair length, and determining the required number of layers of CFRP composite.

2 BACKGROUND OF DAMAGED COLUMNS

Three different repair design methods were developed in this study for five RC columns that were severely damaged under different loading conditions (see Table 1). The as-built cantilever columns were 1/2 scale bridge columns with the same geometry and reinforcing configurations and designed based on CALTRANS [27] and ACI 318 [28] seismic provisions (see Figure 1). The shear span-to-depth ratio (L/b) was 6, where L and b are the length of the column and the cross-section dimension, respectively. The column had a 22 in. (560 mm) square cross section that was reinforced with four No. 9 (29 mm dia.) deformed bars in the corners and eight No. 8 (25 mm dia.) intermediate bars, with a longitudinal reinforcement ratio of 2.13%. Tie reinforcement consisted of square and octagonal No. 3 (10 mm dia.) deformed bars spaced at 3.25 in. (82 mm), with a transverse reinforcement ratio of 1.32%. All reinforcing bars were ASTM A307 Grade 60 (414 MPa), and the design compressive strength of the concrete was 5,000 psi (34 MPa).

In the experimental tests, the five columns were tested to failure under pseudo-static reversed cyclic lateral loading and a constant axial load of approximately 150 kips (667 kN) to simulate the dead load from the superstructure. Column 1 was subjected to cyclic uniaxial cantilever bending and shear (torsional moment -to-bending moment ratio T/M=0) in addition to the constant axial load. Columns 2, 3, and 4 were subjected to the constant axial load and a combined cyclic loading effect of uniaxial cantilever bending, shear, and torsion, with T/M of 0.2, 0.4, and 0.6, respectively. Column 5 was tested under pure torsion (T/M=∞) in addition to the constant axial load. Additional information on the loading protocol is provided in [8].

Table 1. Repair design methodology categories

	Design Action			
	Axial	Shear	Bending	Torsion
Design 1 (Column 1)	×	×	×	
Design 2 (Column 5)	×			×
Design 3 (Columns 2, 3, and 4)	×	×	×	×

As reported in [8], the original columns were tested until either the lateral or the torsional capacity dropped to less than 50% of the peak value. Due to large lateral displacements and/or torsional rotations applied to the columns, severe damage such as concrete core crushing, longitudinal bar buckling, or transverse reinforcing bar opening was observed for all columns. With increasing T/M ratio, the concrete cover spalling height ranged from 25 in. (635 mm) (Column 1) to 120 in. (3050 mm) (Column 5); and the center of the region of concrete core crushing ranged from 10 in. (260 mm) (Column 1) to 64 in. (1620 mm) (Column 5) above the base of the column [23]. The peak lateral load and

torsional moment from the original tests are listed in Table 2.

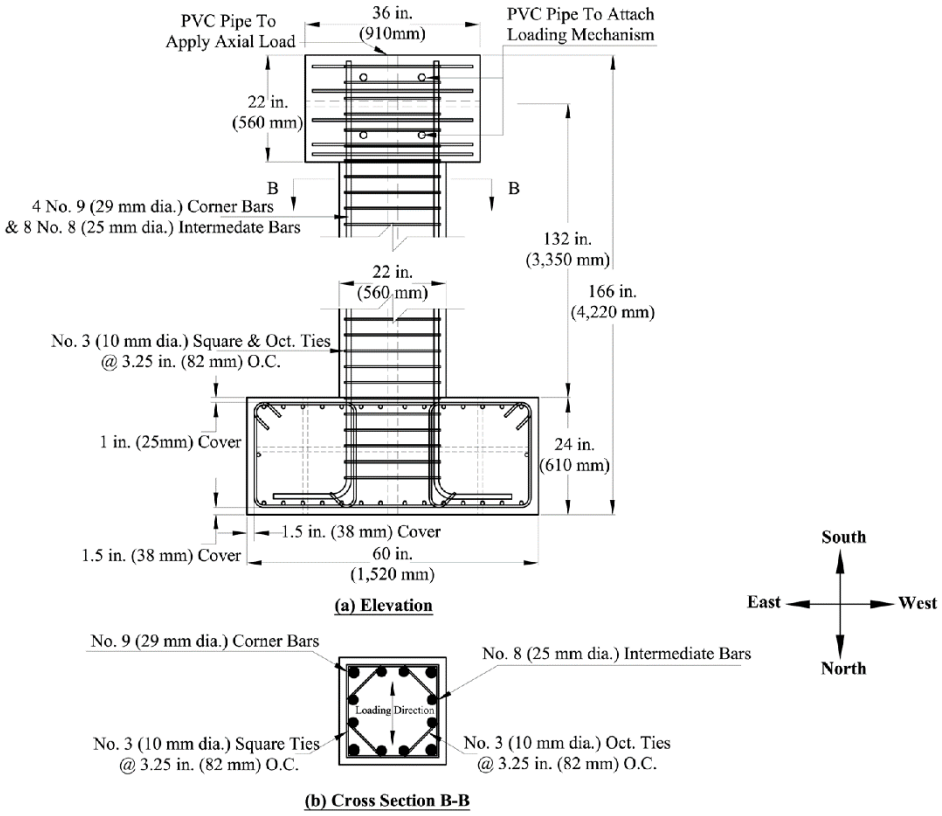

Figure 1. Geometry and reinforcement details of original columns

Table 2. Values of peak lateral load and torsional moment for original columns [23]

Column ID	Lateral Load, kip (kN)	Torsional Moment, kip-ft (kN-m)
1	65 (289)	Not Applicable
2	55 (245)	153 (207)
3	50 (222)	200 (271)
4	51 (227)	179 (243)
5	Not Applicable	243 (330)

3 RERAIR DESIGN METHODOLOGY

3.1 Repair objective

The objective of the rapid repair in this study was to restore the strength to the original condition in flexure, shear, and torsional moment while maintaining or

improving as much ductility and stiffness as possible. The repair was to be completed within a 72-hour period from initiation of the repair work to testing of the repaired specimen.

3.2 Repair procedure

Considering the damage introduced from previous tests discussed in Section 2 and the repair objective stated in Section 3.1, the designated repair procedure included removal of loose concrete, removal of damaged reinforcement that was in the way of the formwork for the repair mortar, erection of formwork, casting and curing of the repair mortar, and application of the CFRP strengthening system to the surface of the column. Details of the repair procedure are described in [23]. No attempt was made to repair the region of the column outside the primary and secondary repair regions.

3.3 Determination of repair length

For columns under bending, a plastic hinge region is usually designated to accommodate large rotations to meet the ductility requirement by seismic design criteria. In this case, damage to concrete and reinforcement is usually concentrated in this same region; thus, the repair length for these columns can be the length of the plastic hinge, which is suggested by Caltrans [27] as 1.5 times the dimension in the direction of bending. However, for columns under combined bending and torsion or torsion alone, the so-called plastic hinge region and the extent of damage along the column length can differ from that of the case under bending alone.

In this study, the plastic hinge length L_p was defined based upon visual observation of the extent of loose concrete (see Table 3). The region of the column near the plastic hinge with cover concrete spalling or crushing was defined as the primary repair region, and the region adjacent to it was defined as the secondary region. To maximize the time efficiency, only the primary and secondary repair regions of the column were repaired (see Figure 2).

Table 3. Length of plastic hinge determined by observation

Column ID	L_p, in., (mm)
1	25 (625)
2	37 (950)
3	58 (1470)
4	94 (2380)
5	120 (3050)

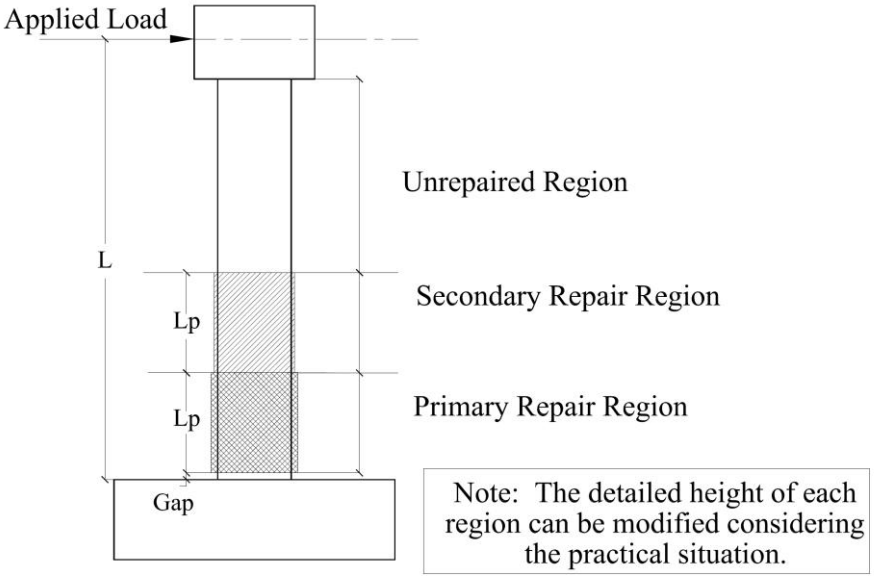

Figure 2. General concept for repair design

3.4 Design of CFRP strengthening system

This section discusses the design of the CFRP strengthening system for Designs 1, 2, and 3 (see Table 1). The CFRP strengthening systems were designed for the primary repair region as defined in Section 3.3. The secondary repair region, with the same length as the primary region, was repaired using half the designed thickness of CFRP used in the primary repair region to prevent shifting of the plastic hinge to the region directly adjacent to the existing plastic hinge. The layout of the CFRP strengthening systems are shown in [23].

The design properties of the dry carbon fiber fabric used in this study were: tensile strength of 550 ksi (3,800 MPa), tensile modulus of 33,000 ksi (227 GPa), ultimate rupture strain of 0.0167, and nominal thickness of 0.0065 in. (0.165 mm) per ply as reported by the manufacturer.

3.4.1 Design 1 for CFRP layout

In Design 1, which was used to repair Column 1 in this study, the CFRP strengthening system was designed to restore the axial, shear, and flexural strength of the column. CFRP sheets with unidirectional fibers parallel to the longitudinal axis of the column were used to restore the flexural strength, whereas CFRP sheets with unidirectional fibers perpendicular to the longitudinal axis (transverse or wrap direction) were used to restore the shear strength and provide confinement. The procedure to design the longitudinal and transverse CFRP is described below.

Step 1: The longitudinal CFRP was preliminarily designed to compensate for the flexural strength loss due to the ruptured longitudinal reinforcing bars by providing the same tensile strength as the yield force of the ruptured bars, which was calculated by Eq. (1):

$$A_s f_y = n t_f w_f f_f \tag{1}$$

where A_s and f_y are the area and yield strength of fractured longitudinal reinforcing bars, respectively; n, t_f, w_f, and f_f are the number of layers, thickness of each layer, width, and fracture strength of the CFRP sheets, respectively.

Step 2: The transverse CFRP was preliminarily designed to restore the shear strength [27] and confinement using Eqs. (2) and (3) according to the provisions used for RC column retrofit [29]. The jacket thickness required for shear was determined as:

$$t_j = \frac{{}^{V_0}/_{\phi} - (V_c + V_s)}{2 \times 0.004 \times E_j \times b} \tag{2}$$

in which V_0 is the over-strength shear, V_c is the concrete shear capacity, V_s is the shear strength provided by the transverse reinforcing steel, ϕ is a strength reduction factor taken as 0.85 for shear, E_j is the CFRP modulus of elasticity, and b is the column dimension in the loading direction. V_0 was taken as the shear corresponding to the maximum moment achieved in the original test (determined from the maximum lateral load given in Table 2). Since four ties in the plastic hinge were opened and removed during placement of the formwork for the repair mortar, which resulted in a larger tie spacing within the plastic hinge region, V_s was conservatively neglected. V_c was calculated based on the estimated compressive strength of the repair mortar at test date, which considered the confinement effect of the transverse CFRP wrap (discussed in Step 3).

The jacket thickness required for confinement was determined as [27]:

$$t_j = \frac{f_l D}{2 \alpha_j E_j \varepsilon_j} \tag{3}$$

where f_l is the confinement stress, and D is the equivalent dimension for the square column. α_j is reduction factor for CFRP modulus of elasticity, and ε_j is the dilating strain estimated to be 0.004 [27].

The total number of layers of transverse CFRP was then determined by the summation of the results given by both Eqs. (2) and (3).

Step 3: Based on the preliminary designs of the longitudinal and transverse CFRP from Steps 1 and 2, a sectional analysis was made to finalize the design. Moment-curvature analysis was conducted using a layer-by-layer approach in which the cross section was divided into a number of discrete layers. Each layer contained a quantity of concrete confined by CFRP, steel ties, or both, longitudinal reinforcing steel, and CFRP. The stresses in the concrete,

reinforcing steel, and CFRP in each layer were determined from the average strain in each layer and the stress-strain relationships. The model by Lam and Teng [30], which is adopted by ACI Committee 440 [31], was used to describe the compressive stress-strain relationship of the CFRP-confined concrete in this study. Though this model has not been verified for damaged concrete confined with FRP, it was used in this design because the damaged concrete would be removed and replaced with repair mortar at the critical cross section where the sectional analysis was conducted. The theoretical moment-curvature relationship for the constant axial load P of 7% of the axial strength was determined by incrementally increasing the concrete strain in the extreme compression layer. For each value of the concrete strain in the extreme compression layer, the neutral axis depth was determined by satisfying force equilibrium as shown in Eq. (4):

$$P = \sum_{i=1}^{m} f_{ci} A_{ci} + \sum_{i=1}^{m} f_{si} A_{si} + \sum_{i=1}^{m} f_{Fi} A_{Fi} \tag{4}$$

where f_{ci}, f_{si}, and f_{Fi} represent the stresses of concrete, steel, and CFRP in the ith layer, A_{ci}, A_{si}, and A_{Fi} are the areas of concrete, steel, and fiber in the ith layer, and m is the number of layers. Then the moment M corresponding to the given concrete strain in the extreme compression layer was determined by taking the moments of the internal forces about a suitable axis using Eq. (5):

$$M = \sum_{i=1}^{m} f_{ci} A_{ci}\, d_{ci} + \sum_{i=1}^{m} f_{si} A_{si}\, d_{si} + \sum_{i=1}^{m} f_{Fi} A_{Fi}\, d_{Fi} - P \cdot \frac{h}{2} \tag{5}$$

where d_i represents the distance of the centroid of ith layer from the extreme compression fiber, and h is the section depth. The curvature was determined by dividing the concrete strain in the extreme compression layer by the neutral axis depth.

3.4.2 Design 2 for CFRP layout

In Design 2, which was used to repair Column 5 in this study, the CFRP strengthening system was designed to restore the axial and torsional strength of the column. The procedure to design the CFRP strengthening system is described below.

Step 1: The torsional strength of an RC member strengthened with externally bonded CFRP was estimated by adding the individual torsional strength contributions of the RC member T_{RC} and the externally bonded CFRP strengthening system T_f as shown in Eq. (6):

$$T = T_{RC} + T_f \tag{6}$$

The contribution of the CFRP was calculated by Eqs. (7) and (8) [32]:

$$T_f = \frac{2A_0 A_f f_{fe}}{s_f} \tag{7}$$

$$\varepsilon_{fe} = 0.004 + \frac{1}{2}\left(\frac{1}{2}\varepsilon_{fu} - 0.004\right) \tag{8}$$

where A_f is the area of CFRP external reinforcement, f_{fe} is the effective CFRP stress = $E_f \varepsilon_{fe}$, s_f is the center-to-center spacing of the applied CFRP sheets, ε_{fe} is the effective CFRP strain, E_f is the modulus of elasticity of CFRP, and ε_{fu} is the ultimate strain of the CFRP system.

Step 2: A nominal amount of CFRP (1 layer) was applied to the surface of the column in the longitudinal direction. The main objective of the longitudinal CFRP was to control concrete crack widths and help maintain the torsional stiffness of the repaired column. Other considerations are discussed in [24].

3.4.3 Design 3 for CFRP layout

In Design 3, which was used to repair Columns 2, 3, and 4 in this study, the CFRP strengthening system was designed to restore the axial, shear, flexural, and torsional strength of the column. Design 3 was conducted based on ACI 318 [28]. The transverse CFRP wrap was designed to restore the shear strength from both lateral load and torque, which considers the interaction between these two effects. The longitudinal CFRP was designed to restore the flexural and torsional strength. Then, the adequacy of the repaired column was checked by considering the interaction of bending and torsion. The procedure to design transverse CFRP is described below.

Step 1: The shear and torsional force demands were determined. Shear: V_u; Torsion: T_u

Step 2: The shear stress from the shear and torsional force demand were determined from Eqs. (9) and (10) [33]:

$$\text{Shear: } v_u = \frac{V_u}{bd} \tag{9}$$

$$\text{Torsion: } v_{tu} = \frac{T_u}{\frac{1}{3}b^3} \tag{10}$$

where b is the cross-sectional width of the column, and d is distance from the column face to the centroid of longitudinal tension reinforcement. To ensure that under combined torsion and shear a diagonal concrete compression failure would be preceded by yielding of the web reinforcement, an upper limit to the combined load should be set. Therefore, the maximum allowable nominal combined stresses were checked using Eq. (11) [33]:

$$v_{u,max} \leq \frac{10\sqrt{f_c'}}{\sqrt{1+(v_{tu}/1.2v_u)^2}} \tag{11}$$

The maximum nominal shear stress that can be carried by the concrete alone in the presence of torsion was calculated by Eq. (12) [33].

$$v_c \leq \frac{2.0\sqrt{f_c'}}{\sqrt{1+(v_{tu}/1.2v_u)^2}} \tag{12}$$

The maximum nominal ultimate torsional stress that can be carried by the concrete alone v_{tc} is related to the calculated v_c by Eq. (13) [33].

$$\frac{v_{tu}}{v_u} = \frac{v_{tc}}{v_c} \tag{13}$$

Step 3: The web reinforcement for shear and torsion was computed. The transverse reinforcement required for shear resistance was calculated by Eqs. (14) and (15).

$$v_u = v_c + v_s \tag{14}$$

$$A_v = \frac{sb}{f_f} v_s \tag{15}$$

where s is the center spacing of the CFRP sheets; v_s is the shear strength provided by shear reinforcement; and f_f is the tensile strength of the CFRP.

Based on (14) and (15), the contribution of the existing transverse reinforcement to the shear strength was conservatively neglected. Transverse reinforcement required to resist torsion was calculated by Eqs. (16), (17), and (18) [32].

$$A_t = \frac{T_f s}{\alpha_t f_f d^2} \tag{16}$$

$$\alpha_t = 0.66 + 0.33 \tag{17}$$

$$T_f = (v_{tu} - v_{tc}) \frac{b^3}{3} \tag{18}$$

Step 4: The total transverse reinforcement needed was taken as the sum of the amounts needed for shear and torsion calculated using Eq. (19).

$$A_{t,total} = \frac{1}{2} A_v + A_t \tag{19}$$

The procedure to design longitudinal CFRP is summarized below:

Step 1: The longitudinal CFRP needed to resist flexural moment A_{lb} was estimated. A sectional analysis was used to determine the longitudinal CFRP required to resist the flexural moment, in which the damaged reinforcement and the confinement effect from the designed transverse CFRP were considered.

Step 2: The longitudinal CFRP needed for torsion was computed. The ACI 318 design equation for stirrups to resist torsion is based on the condition that at least an equal number of longitudinal bars will be provided, therefore, Eq. (20) was used to calculate the longitudinal CFRP needed to resist torsion [28].

$$A_{lt} = 2A_t \frac{2d}{s} \tag{20}$$

Step 3: The total longitudinal CFRP needed was taken as the sum of the CFRP needed to resist flexural moment and torsional moment as shown in Eq. (21):

$$A_{l,total} = A_{lb} + A_{lt} \tag{21}$$

Step 4: The adequacy of the repaired column was checked by considering the

interaction of bending and torsion.

Based on the designed transverse and longitudinal CFRP, the flexural and torsional capacity of the repaired columns was obtained. Then, an interpolated parabolic interaction relationship for pure torsion and pure flexure was used to check the adequacy using Eq. (22) [33].

$$\left(\frac{T_u}{T_{u0}}\right)^2 = 1 - \frac{M_u}{M_{u0}} \tag{22}$$

where T_u is the maximum torsional moment resisted by the original column; T_{u0} is the calculated torsional capacity of the repaired column.

4 EXPERIMENTAL VALIDATION AND DISCUSSION

4.1 Test setup and procedure

The repaired columns were tested under the same initial combined loading effects as the original columns. The test setup for both original and repaired columns is shown in Figure 3. Similar to the procedure used for testing the original columns, the testing procedure for repaired columns was initiated in force control and then continued in displacement control. In testing the original columns, testing shifted to displacement control when first yield of the reinforcing steel occurred [8]. For the repaired columns, yielding of the steel had occurred during the previous test, and monitoring the strain was not always possible due to damage to the strain gages mounted to the reinforcement.

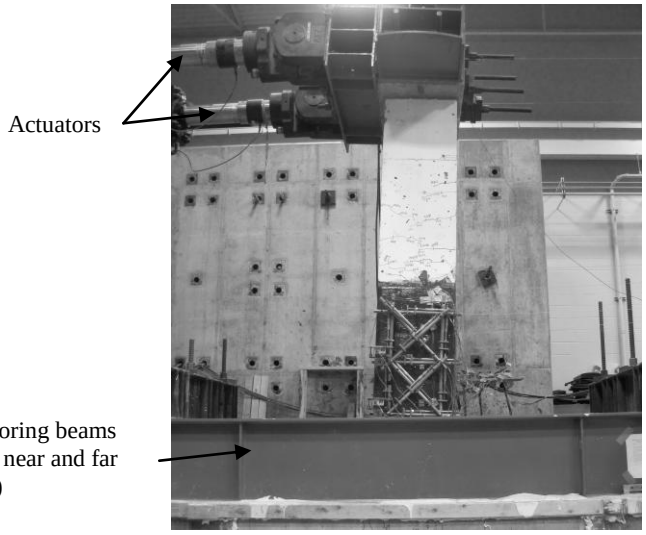

Figure 3. Test setup for columns

Therefore, testing was shifted to displacement control when significant reduction of the stiffness was observed. In addition, different procedures were

used to maintain the torque-to-moment ratio (T/M) during the displacement control testing. In the original tests, an iterative feedback system was used to control the torque-to-moment [8], whereas in the present program, a trial-and-error method was used based on values recorded from the previous cycle. As a result, some differences existed in the loading protocol details.

4.2 Results and discussion

The effectiveness of the repair design was evaluated based on the experimental test results in terms of strength, stiffness, and ductility from the envelope of the lateral load – displacement and torsional moment – twist responses provided in [23]. For clarification, the repaired columns were identified with a suffix "-R" to the IDs of original columns. For example, "Column 1-R" represents the repaired specimen for the damaged Column 1.

The strength of the column was defined herein as the maximum measured applied load during the test [23]. The ratio of the repaired column strength to the original column strength is defined as the strength index *STRI*, which was determined by Eq. (23).

$$STRI = \frac{V_r}{V_o} = \left(\frac{T_r}{T_o}\right) \tag{23}$$

V_r (T_r) and V_o(T_o) in Eq. (23) represent the maximum lateral load (torsional moment) measured in the repaired and original columns, respectively.

The strength indices for the columns are provided in Figure 4, which illustrates that the repair method is effective in restoring the bending and/or torsional strength. The flexural strength restoration ranged from 63-111%, and torsional strength restoration ranged from 83-118%. Although Column 1-R was restored to 75% of its original flexural strength, the results can be misleading since the strength restoration was limited by the flexural capacity of the repaired cross-section with fractured bars, because the longitudinal CFRP failed prematurely when it was pierced by the sharp edge of the anchoring plate, which prompted modifications to the detailing of the anchoring plate (additional discussion on the failure mode of Column 1-R is provided in [22]). For Columns 2-R, 3-R, and 4-R, which were subjected to combined bending and torsion, either the flexural strength, the torsional strength, or both, were fully restored. Bending-torque interactions played a role in the level of bending and torsional strength restored as discussed in the previous sections. For Column 5-R subjected to pure torsion, the torsional strength was fully restored.

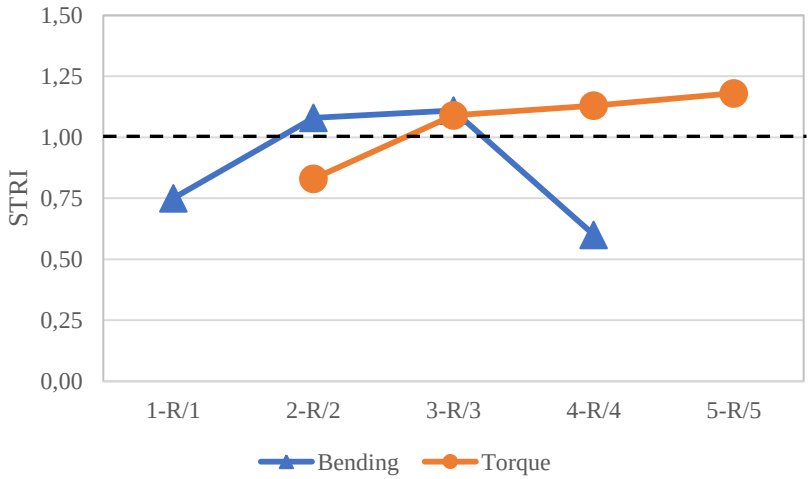

Figure 4. Strength indices (*STRI*) for repaired columns

The stiffness of columns can be expressed by the initial stiffness and the general service stiffness, which were determined by the following methods. The initial stiffness was determined by the ratio of the summation of absolute values of positive and negative peak lateral load (torque for torsion) in the first cycle of the test to the summation of corresponding absolute values of positive and negative displacement (twist for torsion) [22], which was calculated by Eq. (24). The ratio of the repaired column initial stiffness to the original column initial stiffness is defined as the stiffness index $STFI_1$, which was computed by Eq. (25).

$$K_i = \frac{V_{p1}+V_{n1}}{D_{p1}+D_{n1}} = \left(\frac{T_{p1}+T_{n1}}{TW_{p1}+TW_{n1}}\right) \tag{24}$$

$$STFI_1 = \frac{K_{ir}}{K_{io}} \tag{25}$$

In Eq. (24), V_{p1} (T_{p1}) is the measured positive peak lateral load (torsional moment) during the first cycle, and D_{p1} (TW_{p1}) is the corresponding lateral displacement (twist). V_{n1} (T_{n1}) is the absolute value of measured negative peak lateral load (torque), and D_{n1} (TW_{n1}) is the absolute value of the corresponding lateral displacement (twist).

The initial stiffness indices for the repaired columns are illustrated in Figure 5a. The initial bending stiffness indices ranged from 39-112%, and initial torsional stiffness indices ranged from 32-81%. With the exception of the bending stiffness of Column 4-R/4, the initial stiffness of the repaired columns was lower than that of the corresponding original columns. This reduction in initial stiffness is due to the unrepaired cracked portions of the repaired columns and material degradation during the original tests.

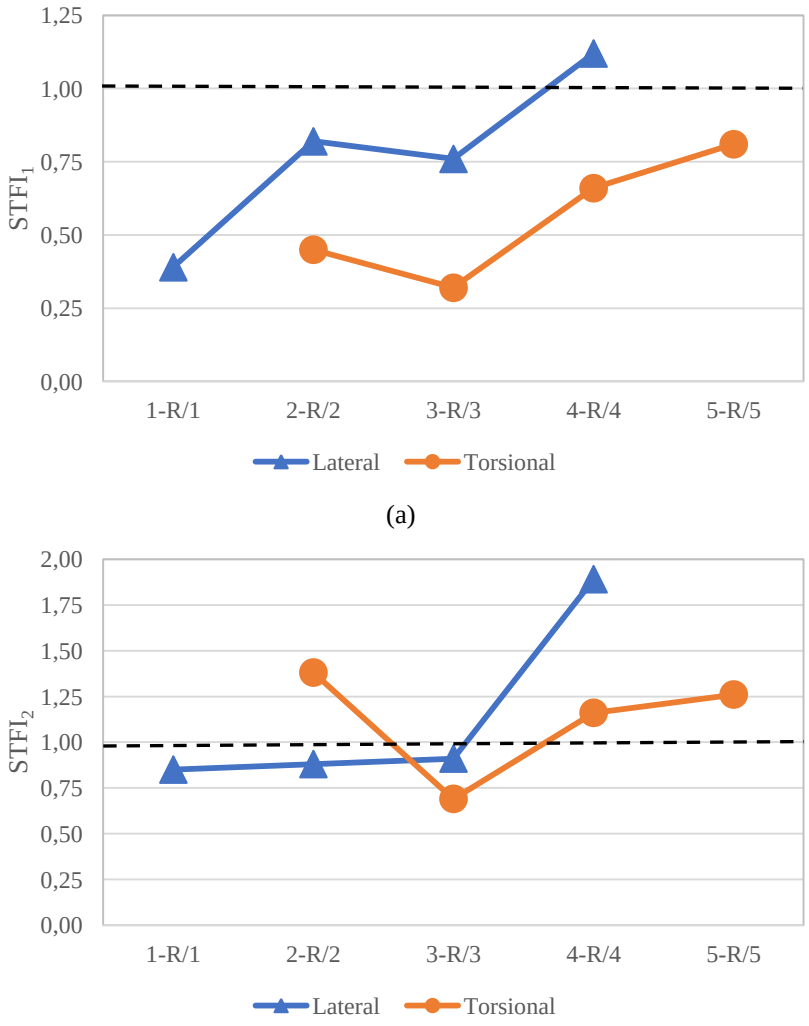

Figure 5. Stiffness indices of initial state ($STFI_1$) (a) and general service ($STFI_2$) (b) for repaired columns.

The general service stiffness index was determined based on an idealized envelope representing an elasto-plastic curve [22] as shown in Figure 6. For the original columns, the envelopes were idealized by setting the initial slope to pass through the first yield point and adjusting the plastic portion so that areas under the measured curve and idealized curve were equal. For the repaired columns, the elastic part of the idealized curve was obtained by connecting the origin to the point on the measured envelope at which the applied load

(torsional moment) was one-half of the peak measured value. The yield level was established by equalizing the area between the measured and idealized curves. The ultimate displacement/twist was defined as the displacement corresponding to a significant drop in the load carrying capacity in bending and/or torsion.

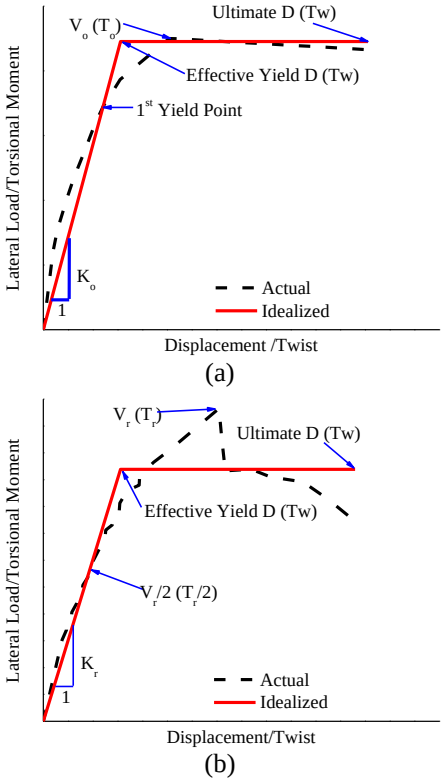

Figure 6. Idealization of lateral load-displacement and torsional moment-twist envelopes of (a) original column and (b) repaired column

The general service stiffness index $STFI_2$ is defined as the ratio of the service stiffness of the repaired column K_r to that of the original column K_o as shown in Eq. (26). The service stiffnesses K_r and K_o are determined from the ratio of the plastic base shear (torque) to the effective yield displacement (twist), which were obtained from the idealized curves (see Figure 5).

$$STFI_2 = \frac{K_r}{K_o} \tag{26}$$

As shown in Figure 5b, the general service stiffness indices for bending ranged from 85-189%, and general service stiffness indices for torsion ranged from 69-138%.

It should be noted that the general service stiffness indices for the repaired columns are dependent on the idealization of the measured envelopes of both original and repaired columns. Results are sensitive to assumptions used in developing the idealized curves. Thus these index values are presented herein to compare the global behaviors of the repaired and corresponding original columns. Also, the torque-bending interaction should be kept in mind in evaluating these indices. In general, the general service stiffness was restored more effectively than the initial stiffness.

The ductility index *DI* is defined as the ratio of the ductility capacity of the repaired column D_r to that of the original column D_o (see Eq. (27)). The ductility capacity is defined as the ratio of the ultimate displacement (twist) to the effective yield displacement (twist), which can be obtained from the idealized curves (see Figure 6).

$$DI = \frac{D_r}{D_o} \tag{27}$$

The ductility indices in terms of both bending and torsion are illustrated in Figure 7. The ductility indices for bending ranged from 68-250%, and torsional ductility restoration ranged from 69-170%.

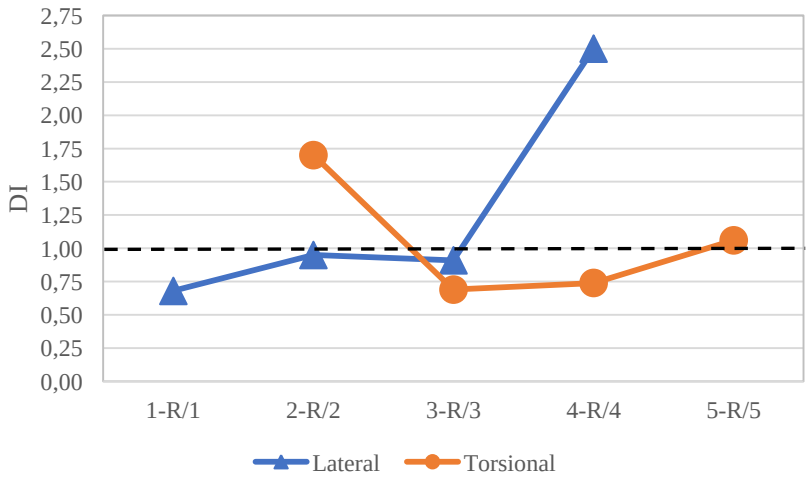

Figure 7. Ductility indices (DI) for repaired columns

Similar to the general service stiffness indices, the ductility indices for the repaired columns are dependent on the idealization of the measured envelopes of both original and repaired columns.

In addition, it should be noted that local modifications (interventions) from the repair of an individual RC bridge column member can change the performance of the member, as demonstrated in this study, which in turn can

influence the performance of the bridge structure. Accordingly, the influence of repair to individual RC bridge columns on the post-repair seismic performance of a bridge system should be investigated. For example, the post-repair seismic peformance of a representtive RC bridge system with repaired column Column 1-R was studied in [34].

5 CONCLUSIONS

This paper presents the repair design methodology for RC bridge columns damaged under combined bending and torsion effects using externally bonded CFRP. The design focuses on the determination of the repair length, and the number of layers of transverse and longitudinal CFRP. Design equations considering different torsional moment-to-bending moment ratios are presented. Five column specimens repaired with CFRP designed by the procedure developed in this study were also tested to validate the effectiveness of the repair design.

Based on the discussion of the testing results, the following conclusions can be made:

- For columns without fractured longitudinal bars, the repair method is effective to a large extent in restoring the lateral and/or torsional strength, service stiffness, and ductility. For the columns in this study without fractured longitudinal bars, the lateral strength, service stiffness, and ductility restoration ranged from 63-111%, 85-185%, and 69-170%, respectively, relative to the original column. The torsional strength, service stiffness, and ductility restoration ranged from 83-118%, 69-138%, and 68-250%, respectively, relative to the original column. Generally, increasing the number of transverse CFRP layers would be an effective way to obtain higher restoration indices, though factors such as bending-torque interaction, failure mode, and repair detailing played a role in the level of strength restored.
- For columns with fractured longitudinal bars, the method utilized in this study was found to be partially successful in restoring the lateral strength, service stiffness, and ductility. For the column in this study with fractured longitudinal bars near the column base, the lateral strength, service stiffness, and ductility restoration were 75%, 85%, and 68%, respectively, relative to the original column. In the case of the column in this study, premature failure of the strengthening system occurred due to detailing of the anchoring system; thus, in order to fully restore the these indices, alternative ways to anchor the longitudinal CFRP or repair the fractured bars should be explored.
- A reduction in initial stiffness after repair was observed due to the previously yielded reinforcing steel and softened concrete, however, the service stiffness was restored or enhanced after repair.

ACKNOWLEDGMENTS

The authors would like to express their appreciation to the University of Missouri Research Board and National University Transportation Center (NUTC) at Missouri S&T (Grant No. DTRT06-G-0014) for financial support for this study.

REFERENCES

[1] Priestley, M. J. N., "Seismic Design and Retrofit of Bridges," John Wiley & Sons, 1996.

[2] Arias-Acosta, J. G., and Sanders, D. H., "Shake Table Testing of Bridge Columns under Combined Actions," In *ASCE & AISC Analysis and Computation Conference/Structur*es Congress/North American Steel Construction Conference (NASCC), Orlando, FL, May, 2010.

[3] Tondini, N., and Bozidar S., "Probabilistic Seismic Demand Model for Curved Reinforced Concrete Bridges," *Bulletin of Earthquake Engineering*, 10(5) 2012, pp: 1455-1479.

[4] Kaviani, P., Zareian, F., and Taciroglu, E., "Seismic behavior of reinforced concrete bridges with skew-angled seat-type abutments," *Engineering Structures*, 45, 2012, pp: 137-150.

[5] Abdelnaby, A. E., Frankie, T. M., Elnashai, A. S., Spencer, B. F., Kuchma, D. A., Silva, P., & Chang, C. M., "Numerical and hybrid analysis of a curved bridge and methods of numerical model calibration," *Engineering Structures*, 70, 2014, pp: 234-245.

[6] Hurtado, G., "Effect of Torsion on the Flexural Ductility of Reinforced Concrete Bridge Columns," PhD Dissertation, University of California, Berkeley, 2010.

[7] Prakash, S., Belarbi A., and You, Y., M.. "Seismic Performance of Circular RC columns Subjected to Axial Force, Bending, and Torsion with Low and Moderate Shear," *Engineering Structures*, 32(1), 2010, pp: 46-59.

[8] Li, Q., and Belarbi, A., "Seismic Behavior of RC Columns with Interlocking Spirals under Combined Loadings Including Torsion," *Procedia Engineering*, 14, 2011, pp: 1281-91.

[9] Nie, J. G., Wang, Y. H., and Fan, J. S., "Experimental Research on Concrete Filled Steel Tube Columns under Combined Compression-Bending-Torsion Cyclic Load," *Thin-Walled Structures*, 67, 2013.

[10] Applied Technology Council (ATC). "Seismic Design Criteria for Bridges and Other Highway Structures: Current and Future," ATC-18, Redwood City, Calif, 1997.

[11] Vosooghi, A., Saiidi, M. S., and Gutierrez, J. "Rapid Repair of RC Bridge Columns Subjected to Earthquakes," *Proceedings of 2nd International Conference on Concrete Repair, Rehabilitation, and Retrofitting (ICCRRR)*, Cape Town, South Africa, 24-26 November, 2008, pp. 1113-1119.

[12] Vosooghi, A., and Saiidi, M. S., "Rapid Repair of High-Shear Earthquake-Damaged RC Bridge Columns," *Proceedings of the 25th US-Japan Bridge Engineering Workshop*, Tsukuba, Japan, Session 7, October, 2009.

[13] Vossoghi, A., and Saiidi, M. S. "Post-Earthquake Evaluation and Emergency Repair of Damaged RC Bridge Columns Using CFRP Materials," *Report Number CCEER-10-05*, September, 2010.

[14] Shin, M., and Andrawes, B., "Emergency Repair of Severely Damaged Reinforced Concrete Columns Using Active Confinement with Shape Memory Alloys," *Smart Materials and Structures*, V. 20, 9pp, 2011.

[15] Parks, J.E., Brown, D.N., Ameli, M.J., Pantelides, C.P., "Seismic Repair of Severely Damaged Precast Reinforced Concrete Bridge Columns Connected with Grouted Splice Sleeves." ACI Structure Journal, 113(3), 2016, pp: 615-626.

[16] Wu, R. Y., and Pantelides, C.P., "Rapid Seismic Repair of Severely Damaged Cast-in-Place Reinforced Concrete Bridge Piers." Transportation Research Board, 96th Annual Meeting, 2017, Paper No. 17-06278.

[17] Wu, R. Y., and Pantelides, C.P., "Rapid Seismic Repair of Severely Damaged Reinforced Concrete Bridge Piers." Proceedings, Structures Congress 2017, p: 371-381.
[18] Matthys, S., Triantafillou, T., "Shear and Torsion Strengthening with Externally Bonded FRP Reinforcement," *ASCE Conf. Specialty Workshop of Composites in Construction Proceedings of the International Workshop*, 2001.
[19] Ghobarah, A., Ghorbel, M. N., Chidiac, S. E., "Upgrading Torsional Resistance of Reinforced Concrete Beams Using Fiber-Reinforced Polymer," *Journal of Composites for Construction*, ASCE, Vol. 6, No. 4, November 1, 2002.
[20] Panchacharam, S., Belarbi, A., "Torsional Behavior of Reinforced Concrete Beams Strengthened with FRP Composites," *First FIB Congress*, Osaka, Japan, October, 2002, 13-19.
[21] Chalioris, C. E. "Torsional Strengthening of Rectangular and Flanged Beams Using Carbon Fiber-Reinforced-Polymers – Experimental Study," *Construction and Building Materials*, 22, 2008.
[22] He, R., Grelle, S., Sneed, L. H., and Belarbi, A., "Rapid repair of a severely damaged RC column having fractured bars using externally bonded CFRP." *Composite Structures*, 101, 2013, pp: 225-242.
[23] He, R., Sneed, L. H. and Belarbi. A., "Rapid repair of severely damaged RC columns with different damage conditions: An experimental study." *International Journal of Concrete Structures and Materials* 7.1, 2013, pp: 35-50.
[24] He, R., Sneed, L. H. and Belarbi. A., "Torsional repair of severely damaged column using carbon fiber-reinforced polymer." *ACI Structural Journal* 111(3), 2014, pp: 705.
[25] Yang, Y., Sneed, L., Saiidi, M.S., Belarbi, A., Ehsani, M. and He, R., "Emergency repair of an RC bridge column with fractured bars using externally bonded prefabricated thin CFRP laminates and CFRP strips." *Composite Structures*, 133, 2015, pp: 727-738.
[26] Yang Y., Sneed L. H., Morgan A., Saiidi M. S., Belarbi A. Repair of RC bridge columns with interlocking spirals and fractured longitudinal bars–An experimental study. *Construction and Building Materials*. 78, 2015, pp: 405-420.
[27] California Department of Transportation (Caltrans), "Seismic Design Criteria Version 1.4," California, USA: Engineering Service Center, Earthquake Engineering Branch, 2006
[28] American Concrete Institute (ACI) Committee 318, "Building Code Requirements for Structural Concrete and Commentary," ACI 318-11, Farmington Hills, Mich, 2011.
[29] California Department of Transportation (Caltrans), "Memo to Designers 20-4 attachment B," California, USA: Engineering Service Center, Earthquake Engineering Branch, 2007.
[30] Lam L., Teng J. Design-Oriented Stress-Strain Model for FRP-Confined Concrete in Rectangular Columns. *Journal of Reinforced Plastic Composites*, 2003; 22(13): 1149-86.
[31] ACI 440.2R-8. Guide for the Design and Construction of Externally Bonded FRP Systems for Strengthening Concrete Structures. American Concrete Institute: Farmington Hills, MI; 2008. p. 76.
[32] Zureick, A. H., Ellingwood, B. R., Nowak, A. S., Mertz, D. R., and Triantafillou, T. C., "Recommended Guide Specification for the Design of Externally Bonded FRP Systems for Repair and Strengthening of Concrete Bridge Elements," NCHRP Report 655. 28-43, Washington, D. C., 2010.
[33] Park, R., Paulay, T., "Reinforced Concrete Structures", John Wiley & Sons, 1975.
[34] He R., Yang Y., Sneed L. H. Post-Repair Seismic Assessment of RC Bridges Damaged with Fractured Column Bars – A Numerical Approach. *Engineering Structures*, 112, 2016, pp: 100-113.